

Correlation of Optical Image Sensor Noise in Space with Trapped Proton Flux

15 May 2003

Prepared by

A. CAMPBELL,¹ J. WEHLBURG,² P. MARSHALL,³
B. BLAKE,⁴ J. FENNELL,⁴ and M. REDDING⁴

¹Naval Research Laboratory, Washington, DC

²Sandia National laboratories, Albuquerque, NM

³NRL Consultant, Brookneal, VA

⁴The Aerospace Corporation, El Segundo, CA

Prepared for

SPACE AND MISSILE SYSTEMS CENTER
AIR FORCE SPACE COMMAND
2430 E. El Segundo Boulevard
Los Angeles Air Force Base, CA 90245


20030616 064

Engineering and Technology Group

This report was submitted by The Aerospace Corporation, El Segundo, CA 90245-4691, under Contract No. F04701-00-C-0009 with the Space and Missile Systems Center, 2430 E. El Segundo Blvd., Los Angeles Air Force Base, CA 90245. It was reviewed and approved for The Aerospace Corporation by J. A. Hackwell, Principal Director, Space Science Applications Laboratory. Michael Zambrana was the project officer for the Mission-Oriented Investigation and Experimentation (MOIE) program.

This report has been reviewed by the Public Affairs Office (PAS) and is releasable to the National Technical Information Service (NTIS). At NTIS, it will be available to the general public, including foreign nationals.

This technical report has been reviewed and is approved for publication. Publication of this report does not constitute Air Force approval of the report's findings or conclusions. It is published only for the exchange and stimulation of ideas.


Michael Zambrana
SMC/AXE

REPORT DOCUMENTATION PAGEForm Approved
OMB No. 0704-0188

Public reporting burden for this collection of information is estimated to average 1 hour per response, including the time for reviewing instructions, searching existing data sources, gathering and maintaining the data needed, and completing and reviewing this collection of information. Send comments regarding this burden estimate or any other aspect of this collection of information, including suggestions for reducing this burden to Department of Defense, Washington Headquarters Services, Directorate for Information Operations and Reports (0704-0188), 1215 Jefferson Davis Highway, Suite 1204, Arlington, VA 22202-4302. Respondents should be aware that notwithstanding any other provision of law, no person shall be subject to any penalty for failing to comply with a collection of information if it does not display a currently valid OMB control number. PLEASE DO NOT RETURN YOUR FORM TO THE ABOVE ADDRESS.

1. REPORT DATE (DD-MM-YYYY) 15-05-2003		2. REPORT TYPE		3. DATES COVERED (From - To)	
4. TITLE AND SUBTITLE Correlation of Optical Image Sensor Noise in Space with Trapped Proton Flux				5a. CONTRACT NUMBER F04701-00-C-0009	
				5b. GRANT NUMBER	
				5c. PROGRAM ELEMENT NUMBER	
6. AUTHOR(S) A. Campbell, J. Wehlburg, P. Marshall, B. Blake, J. Fennell, M. Redding				5d. PROJECT NUMBER	
				5e. TASK NUMBER	
				5f. WORK UNIT NUMBER	
7. PERFORMING ORGANIZATION NAME(S) AND ADDRESS(ES) The Aerospace Corporation Laboratory Operations El Segundo, CA 90245-4691				8. PERFORMING ORGANIZATION REPORT NUMBER TR-2003(8570)-8	
9. SPONSORING / MONITORING AGENCY NAME(S) AND ADDRESS(ES) Space and Missile Systems Center Air Force Space Command 2450 E. El Segundo Blvd. Los Angeles Air Force Base, CA 90245				10. SPONSOR/MONITOR'S ACRONYM(S) SMC	
				11. SPONSOR/MONITOR'S REPORT NUMBER(S) SMC-TR-03-16	
12. DISTRIBUTION/AVAILABILITY STATEMENT Approved for public release; distribution unlimited.					
13. SUPPLEMENTARY NOTES					
14. ABSTRACT MPTB particle environment measurements are being correlated with noise signals in a CMOS visible sensor to model interactions of particles and pixel sensor elements.					
15. SUBJECT TERMS					
16. SECURITY CLASSIFICATION OF:			17. LIMITATION OF ABSTRACT	18. NUMBER OF PAGES 7	19a. NAME OF RESPONSIBLE PERSON Joe Fennell
a. REPORT UNCLASSIFIED	b. ABSTRACT UNCLASSIFIED	c. THIS PAGE UNCLASSIFIED			19b. TELEPHONE NUMBER (include area code) (310)336-7075

Acknowledgments

The authors would like to thank Maurice Wilkinson, Glenn Berg, and Ron Elsen of Boeing; and Jeannette Garza of MIT for the technical help and support in this work.

Contents

Summary & Introduction	1
Modeling.....	2
Conclusions	3
References	7

Figures

1. Maximum row pixel noise signal above average & proton & electron flux vs UT – 30 September 2002.	3
2. Length distribution histogram of rays less than 1000 mils.....	4
3. Calculated incident proton spectra incident and penetrating (650 mils) the TX instrument striking the sensor	4
4. Pixel noise signal frame average and maximum vs UT – 30 September 2002.....	5
5. Output from the TX sensor while dark measurements were made outside of the proton belts (top, a) and during a proton belt traversal (bottom, b).....	6

Summary & Introduction

MPTB is flying in a highly elliptical HEO orbit that passes through the proton belts. The CMOS active pixel optical sensor in a related experiment (called TX) shows increased noise levels during proton belt passages so noise signals above background can be attributed to the deposition and collection of charge from protons. Another related experiment flying with MPTB is a particle detector which measures, among other items, proton flux. This work reports correlations of pixel noise and proton flux in order to quantify the response of the sensor elements to a measured proton spectrum. This is done through modeling of radiation transport to the sensor elements with a detailed knowledge of the design and fabrication of the sensor. These results will then be used to predict the response of more modern optical sensors to proton environments.

The MPTB orbit is very close to 12 hours in duration; the perigee is about 1000 km, while apogee is beyond geo-synchronous. Nearly 9 hours of the orbit are in deep space, with the remaining 3.5 hours comprised of a rapid drop to perigee and climb back to deep space. Thus the orbital path transits directly through the proton belts twice each orbit. Details of the orbit can be found in Dyer et.al.[1]

An instrument flying with MPTB is being utilized to provide measurements of the radiation environment at the same time the measurements are being made on the sensor. It is the Aerospace DSU (Dose Simetry Unit) instrument. The DSU measures proton fluxes in four energy regions and dose behind several shield thicknesses over a hemispherical geometry. For this work, the proton fluxes with energies greater than 6.5, 15 and 25 MeV are being analyzed. The DSU instrument is described in detail in references[2-7]. Figure 1 includes DSU proton flux data for one orbit segment near perigee on 30 September 2002. Data is taken approximately each 15 seconds.

Measurements were made using the TX instrument during proton belt passes. The signals analyzed were due to inherent noise in the sensor and related electronics and interactions with the radiation environment. Sequential reads row-by-row are performed and this data is what is used in this analysis. Data in this summary represent arbitrary noise signals but in the full paper this will be converted to electron-hole pairs using the overall gain and sensitivity of instrument.

The visible sensor data described in this summary in the TX instrument were acquired using a Rockwell TCM2620V monolithic silicon sensor array fabricated in a 0.6 micrometer CMOS process. The sensor has elements with a 40 micrometer pitch, a 30% active area, and a depletion thickness of 12 micrometers. The format is 256 x 256 pixels with multiplexed snapshot mode Capacitive Trans-Impedance Amplifier (CTIA) readout. Unit cell area was divided between the CTIA elements, including a 0.4 pF capacitor, and implanted n-on-p diode structures for optical detection. The sensor includes on-chip clock and bias generators as well as column and row buffering, and four high-speed class A-B amplifier outputs. With operation at room temperature, the read noise was typically 30 electrons with a 3-volt maximum signal. Further descriptions of the n-on-p detector optical characteristics and circuit performance will be provided in the full paper.

Proton testing was performed on samples of the TCM2620V array, and the device was found to be insensitive to proton induced latchup. Also, on-orbit flight data will be compared with the measured response and modeling with 60 MeV protons incident with a flux of 8.54×10^6 p/cm²/s at a 15 Hz readout rate. Additional details of the laboratory test detail and measurements will be provided in the full paper.

Modeling

The host vehicle and the TX experiment were modeled with the Air Force Research Laboratory radiation modeling code SVC[8]. The effective average shielding, in terms of 528 aluminum equivalent rays, was determined to be about 650 mils of aluminum about the TX sensor. The distribution shows 177 of these are 1000 mils or less. Figure 2 shows the distribution of these rays. Although the DSU provides the trapped proton spectra for protons above 25 MeV, only incident protons of greater than 65 MeV can reach the sensor. The AP-8min flux map was used to generate the high-energy portion of the incident proton flux at the sensor location. Figure 3 shows the incident and penetrating flux, integral in energy, at the sensor location for the first proton peak of Figure 1. Clearly the sensor shielding results in a hard proton energy spectrum at the sensor. A more detailed shielding analysis to consider the sensor orientation and possible directional effects from the shielding will be performed for the presentation and paper. Proton spectra at four shield thicknesses, 460 (minimum), 650, 1000 and 2000 mils equivalent Al will be used for the analysis.

In addition to the DSU proton flux measurements, Figure 4 also shows the largest pixel noise signals for the same time period. Rows of 170 pixels, a segment of the 256 cells per row, are sampled four at a time approximately each 1.8 seconds and the figure shows the largest value among the 170 in arbitrary units. The average noise level inherent in the sensor is 4.4.

Figure 5 shows dark frames, no light input, of on-orbit taken during two portions of an orbit. The top figure a shows an image taken outside of the proton belts and the bottom figure b shows an image taken during a proton belt passage. This data is histogrammed and converted to charge carrier for the analysis. This will then be used in the modeling.

In the full paper we will provide detailed predictions of the expected array response relative to the trapped proton environment after transport through surrounding structures. Due to the confinement of the n-on-p diode to the epitaxial layer, we model the charge collection as a combination of drift with some contribution from diffusion within the 12 micrometer epitaxial layer. Assuming a 12 micrometer depletion depth, the resulting charge due to a strike by a trapped proton is typically several thousand electrons, with the charge yield depending on proton energy, trajectory, and to some extent the carrier lifetime in the epitaxial layer. Also, since the implanted diode occupies only a portion of the unit cell, we do not expect charge sharing between adjacent pixels due to diffusion. The paper will

describe both in measured array response and model predictions, that adjacent pixels are affected only when proton trajectories result in transport through neighboring detector elements.

Our approach to modeling the interactions between transported protons and the pixel level response is based on a computational tool that was described by Pickel [7]. Modifications from the cited application to infrared detectors include the incorporation of the Si detector material, and geometries appropriate to monolithic detection in a CMOS implanted diode. The model employs a combination of analytic and Monte Carlo techniques to track ion deposited charge as it is collected via both drift and diffusion in a two dimensional array. Structural dependent spectral characteristics of the transported environment with detailed descriptions of trajectories are incorporated in the modeling approach. Further details of the model and comparisons between modeled and measured results will be presented in the full paper.

Conclusions

This work will show the correlations in space between measured particle flux and spectrum and the noise interactions of a CMOS image sensor pixel. This will be done using ray-tracing modeling including a detailed analysis of the sensor design.

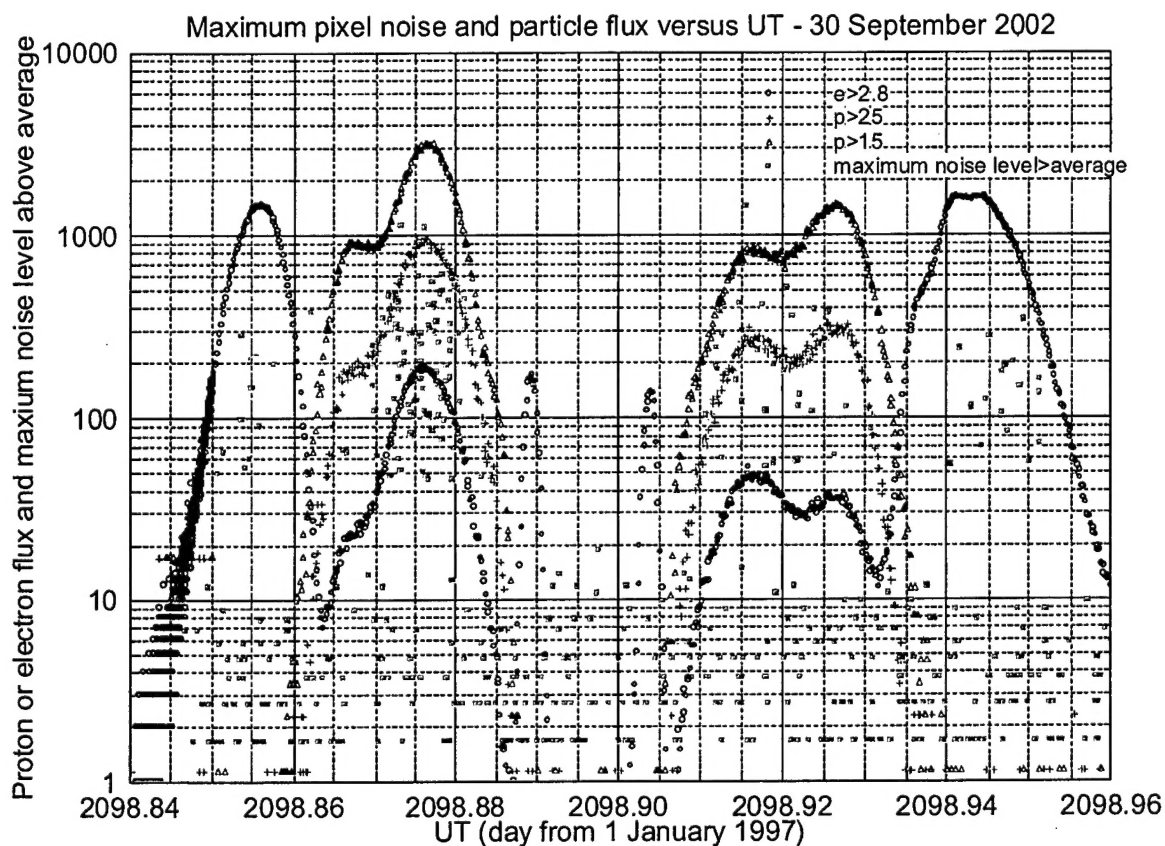


Figure 1: Maximum row pixel noise signal above average & proton & electron flux vs UT - 30 September 2002.

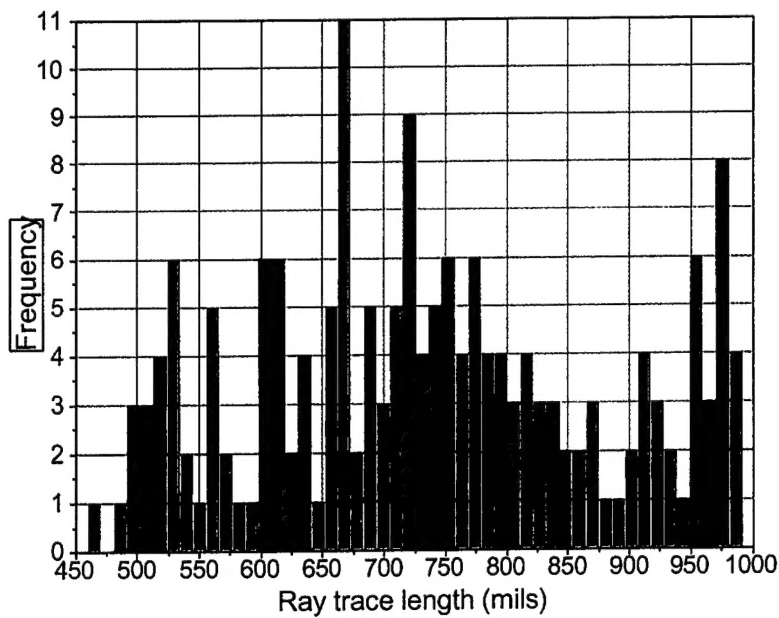


Figure 2: Length distribution histogram of rays less than 1000 mils.

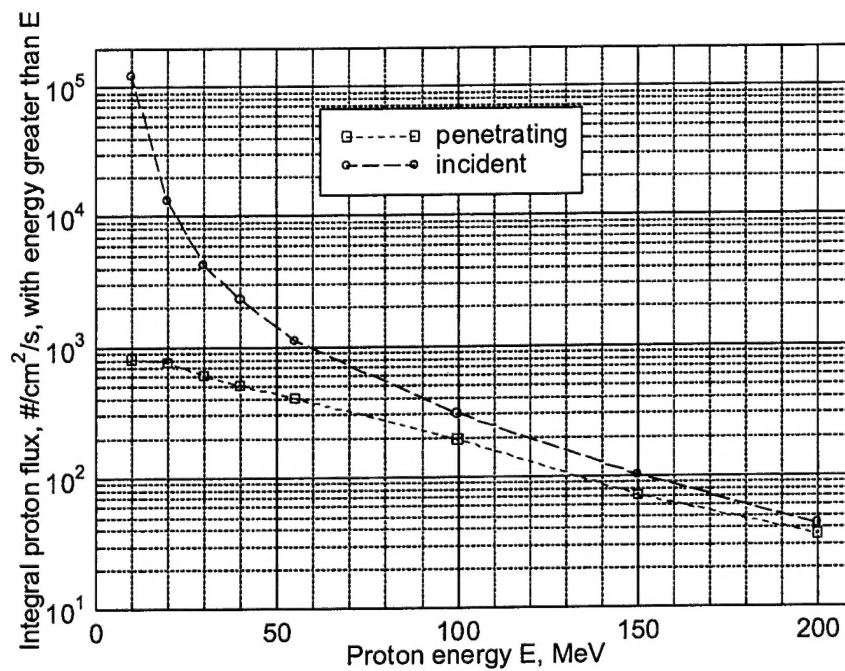


Figure 3 – Calculated incident proton spectra incident and penetrating (650 mils) the TX instrument striking the sensor.

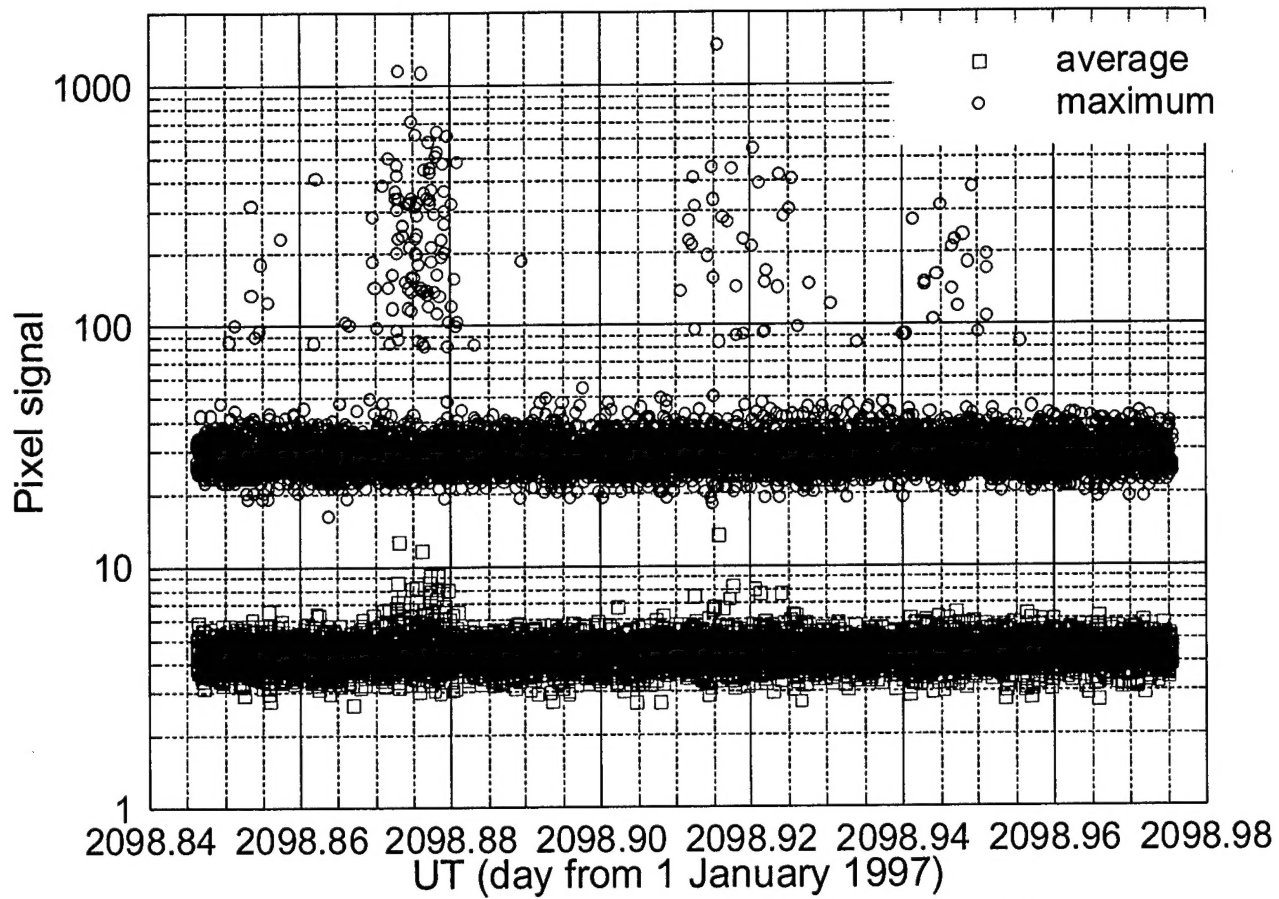


Figure 4: Pixel noise signal frame average and maximum vs UT - 30 September 2002

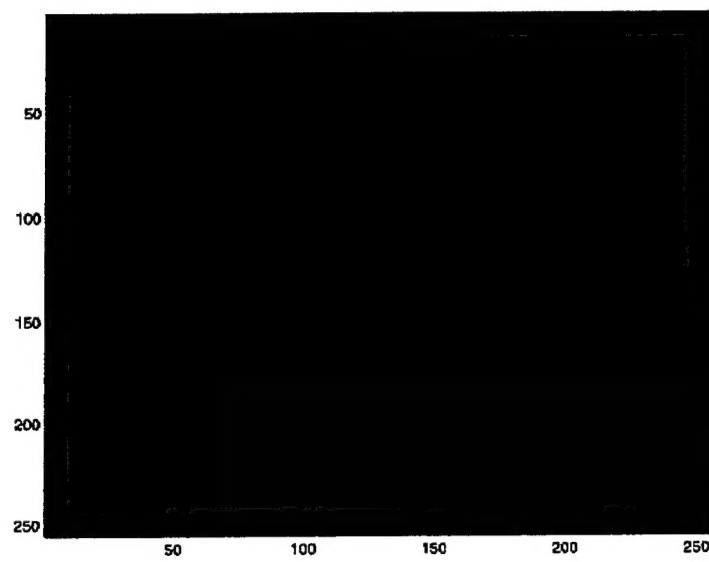
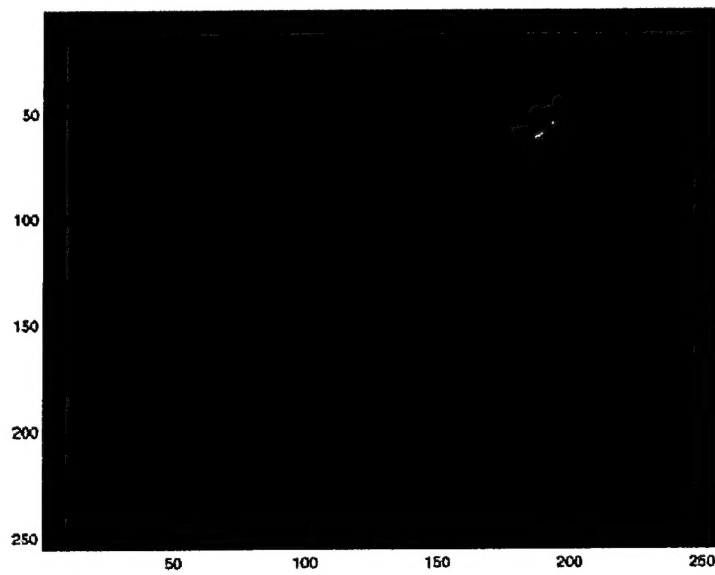


Figure 5a & 5b: The two figures above show output from the TX sensor while dark measurements were made outside of the proton belts (top, a) and during a proton belt traversal (bottom, b).

References

1. C. Dyer, P. Truscott, C. Sanderson, C. Watson, C. Peerless, P. Knight, R. Mugford, T. Cousins and R. Noulty, "Radiation Environment Measurements from CREAM & CREDO during the Approach to Solar Maximum," IEEE Trans. Nucl. Sci NS-47, pp 2208-2217, December 2000
2. Blake JB, Baker DN, Turner N, Ogilvie KW, Lepping RP, "Correlation of changes in the outer-zone relativistic-electron population with upstream solar wind and magnetic field measurements," GEOPHYSICAL RESEARCH LETTERS 24 (8): 927-929 APR 15 1997
3. Fennell JF, Koons HC, Chen MW, Blake JB, "Internal charging: A preliminary environmental specification for satellites," IEEE Transactions on Plasma Science 28 (6): 2029-2036, December 2000.
4. Fennell, J. F., J. B. Blake, J. L. Roeder, R. Sheldon, and H. Spence, "Tail Lobe and Open Field Line Region Entries at Mid to High Latitudes," Adv. Space Res, 20, 431-435, 1997.
5. Fennell, J. F., H. C. Koons, J. L. Roeder, and J. B. Blake, Spacecraft Charging: Observations and Relationship to Satellite Anomalies, proceedings of 7th Spacecraft Charging Technology Conference, ESA SP-476, 279, November 2001.
6. Mazur, J. E., "The Radiation Environment Outside and Inside a Spacecraft," Section II of "Radiation Effects - From Particles to Payloads," 2002 IEEE NSREC Short Course Notebook.
7. Radiation-Induced Charge Collection in Infrared Detector Arrays, J.C. Pickel, Robert A. Reed, R. Ladbury, B. Raucher, Paul W. Marshall, Tom M. Jordan, B. Fodness, and G. Gee, IEEE TNS, Vol. 49, No. 6, pp. 2822-2829.
8. Smith, N, "Satellite Vulnerability Codes Users Manual," WL-TR-90-70, November 1990.

LABORATORY OPERATIONS

The Aerospace Corporation functions as an "architect-engineer" for national security programs, specializing in advanced military space systems. The Corporation's Laboratory Operations supports the effective and timely development and operation of national security systems through scientific research and the application of advanced technology. Vital to the success of the Corporation is the technical staff's wide-ranging expertise and its ability to stay abreast of new technological developments and program support issues associated with rapidly evolving space systems. Contributing capabilities are provided by these individual organizations:

Electronics and Photonics Laboratory: Microelectronics, VLSI reliability, failure analysis, solid-state device physics, compound semiconductors, radiation effects, infrared and CCD detector devices, data storage and display technologies; lasers and electro-optics, solid-state laser design, micro-optics, optical communications, and fiber-optic sensors; atomic frequency standards, applied laser spectroscopy, laser chemistry, atmospheric propagation and beam control, LIDAR/LADAR remote sensing; solar cell and array testing and evaluation, battery electrochemistry, battery testing and evaluation.

Space Materials Laboratory: Evaluation and characterizations of new materials and processing techniques: metals, alloys, ceramics, polymers, thin films, and composites; development of advanced deposition processes; nondestructive evaluation, component failure analysis and reliability; structural mechanics, fracture mechanics, and stress corrosion; analysis and evaluation of materials at cryogenic and elevated temperatures; launch vehicle fluid mechanics, heat transfer and flight dynamics; aerothermodynamics; chemical and electric propulsion; environmental chemistry; combustion processes; space environment effects on materials, hardening and vulnerability assessment; contamination, thermal and structural control; lubrication and surface phenomena. Microelectromechanical systems (MEMS) for space applications; laser micromachining; laser-surface physical and chemical interactions; micropropulsion; micro- and nanosatellite mission analysis; intelligent microinstruments for monitoring space and launch system environments.

Space Science Applications Laboratory: Magnetospheric, auroral and cosmic-ray physics, wave-particle interactions, magnetospheric plasma waves; atmospheric and ionospheric physics, density and composition of the upper atmosphere, remote sensing using atmospheric radiation; solar physics, infrared astronomy, infrared signature analysis; infrared surveillance, imaging and remote sensing; multispectral and hyperspectral sensor development; data analysis and algorithm development; applications of multispectral and hyperspectral imagery to defense, civil space, commercial, and environmental missions; effects of solar activity, magnetic storms and nuclear explosions on the Earth's atmosphere, ionosphere and magnetosphere; effects of electromagnetic and particulate radiations on space systems; space instrumentation, design, fabrication and test; environmental chemistry, trace detection; atmospheric chemical reactions, atmospheric optics, light scattering, state-specific chemical reactions, and radiative signatures of missile plumes.